Leukoencephalopathy, cerebral calcifications, and cysts: New observations

L. M. Nagae-Poetscher, G. Bibat, M. Philippart, S. Rosemberg, A. Fatemi, M. T.C. Lacerda, M. O.R. Costa, F. Kok, C. Costa Leite, A. Horská, P. B. Barker and S. Naidu

Neurology 2004;62;1206-1209

Leukoencephalopathy, cerebral calcifications, and cysts

New observations

L.M. Nagae-Poetscher, MD; G. Bibat, MD; M. Philippart, MD; S. Rosemberg, MD; A. Fatemi, MD; M.T.C. Lacerda, MD; M.O.R. Costa, MD; F. Kok, MD; C. Costa Leite, MD, PhD; A. Horská, PhD; P.B. Barker, DPhil; and S. Naidu, MD

Abstract—We describe three cases of the rare syndrome of leukoencephalopathy, brain calcifications, and cysts. Conventional MRI, proton spectroscopy, and diffusion-weighted imaging yielded additional information on the disease. Imaging findings favor increased water content rather than a demyelinating process in the pathophysiology of this disease. Clinical features of Coats disease and consanguinity were also encountered.

NEUROLOGY 2004;62:1206–1209

Traditionally, diagnosis and classification of leukoencephalopathies have relied on clinical, genetic, biochemical, or histopathologic findings. MRI, along with spectroscopy (MRS) and diffusion-weighted imaging (DWI), has provided additional insight into the pathology of the disease.

We report three patients with the rare syndrome of leukoencephalopathy, brain calcifications, and cysts[1] (LCC) and describe additional clinical features using contrast-enhanced MRI, MRS, and DWI.

Case reports. *Case 1.* Patient 1 is a 12-year-old boy with (negative) unremarkable family and prenatal history. He was normal until age 2.5 years, when he developed slowly progressive dystonia, spasticity, and ataxia, with relative preservation of social skills. Sparse pale hair and dyspigmented skin areas were noticed in the neck, face, scalp, and groin. Laboratory investigation revealed normal G-banded chromosomal studies (band resolution of 425). Aminoaciduria, organoaciduria, and lysosomal, peroxisomal, and celiac diseases were excluded. Serum calcium, phosphate, and alkaline phosphatase were normal. At age 6 years, CSF showed 18 mg/dL protein and no cells or lactate. Muscle electron microscopy study, mitochondrial enzymes, and DNA mutation analyses were normal. Ophthalmologic examination revealed Coats disease. Cerebral angiography and magnetic resonance angiography (MRA) were normal. Brain CT and MRI (figures 1 and 2.I) were strikingly similar to other cases described in this report (all examinations were performed using a 1.5-T magnet), showing diffuse leukodystrophy, relatively sparing the U fibers and corpus callosum (see figure 1, A and B), with extensive coarse calcifications (see figures 1E and 2.IA) in the basal ganglia, thalamus, subcortical white matter, and dentate nuclei. Presence of an interhemispheric cyst, distinct from the pineal gland, was noted (see figure 1, B through D, F, and G). Subtle enhancement was observed in the deep white matter, lining of cyst wall, and adjacent to the calcifications (see figure 1, F and G).

Case 2. Patient 2 is a 9-year-old girl, whose family and perinatal history are noncontributory. She had normal development until age 2 years, despite an episode of apnea on day 2 of life. She developed slowly progressive right hemiplegia with diffuse spasticity, dystonia, ataxia, and cognitive delay. Laboratory investigation disclosed normal plasma amino acids and urine amino and organic acids. CSF neurotransmitters (5-hydroxyindolacetic acid, homovanillic acid, and 3-O-methyldopa), cell count (10 erythrocytes; no leukocytes), and biochemistry (55 mg/dL of glucose; 33 mg/dL of proteins; and normal lactate) at age 7 years, EMG, brain auditory evoked response (BAER), eye examination, serum calcium, lactate, and pyruvate were normal. Brain CT and MRI were similar to those seen in Patient 1. Of note, the calcifications and the interhemispheric cyst were not seen on a CT performed on day 5 of life.

Case 3. Patient 3 is a 14-year-old girl born to consanguineous parents. She had low birth weight (2.3 kg), seizures, static encephalopathy, and microcephaly. After a 4-month history of headache and vomiting from intracranial hypertension, she revealed spasticity, ataxia, dystonia, bulbar signs, and papilledema. CT and MRI showed similar leukoencephalopathy and calcifications associated with obstructive hydrocephalus from a posterior fossa cyst (see figure 2.I, A, D through F). Biopsy from a small fragment of the cyst wall revealed dense, poorly cellular, fibroglial tissue with abundant Rosenthal fibers (figure 2.II). Despite the presence of macrophages filled with ferric iron deposits around the majority of the vessels and few vessels partially calcified, no definite angiomatous changes were seen.

MRS and DWI. MRS of Patient 2 revealed no lactate, reduced N-acetylaspartate (NAA), and slightly increased creatine (Cr) in frontal and parietal regions.[2] However, choline (Cho) was reduced only in parietal regions (figure 3). No metabolites were detected in the interhemispheric cyst or within the calcifications.

In Patient 3, a single-voxel (SV) MRS study with an 8-cm^3 voxel located in the affected left parieto-occipital white matter showed low NAA:Cr (1.61 for PRESS [repetition time (TR)/echo time (TE), 1,500/135 ms]; 0.88 for STEAM [TR/TE, 1,500/30 ms]) and Cho:Cr (0.81 for PRESS; 0.78 for STEAM) peak ratios. Average values, obtained from four normal age-matched control subjects from the same institution, showed NAA:Cr ratios of 2.37 $\pm$ 0.02 (PRESS) and 1.51 $\pm$ 0.06 (STEAM) and Cho:Cr ratios of 1.32 $\pm$ 0.20 (PRESS) and 0.93 $\pm$ 0.11 (STEAM).

From The Russell H. Morgan Department of Radiology and Radiological Science (Drs. Nagae-Poetscher, Horská, and Barker), Johns Hopkins University School of Medicine, Baltimore, MD; Kennedy Krieger Institute (Drs. Nagae-Poetscher, Bibat, Fatemi, and Naidu), Baltimore, MD; UCLA, MRRC, and BRI (Dr. Philippart), Los Angeles, CA; and Hospital das Clínicas da Faculdade de Medicina da Universidade de São Paulo (Drs. Rosemberg, Lacerda, Costa, Kok, and Costa Leite), São Paulo, Brazil.

Supported by a resource grant from the National Center for Research Resources (RR15241).

Received June 26, 2003. Accepted in final form November 10, 2003.

Address correspondence and reprint requests to Dr. S. Naidu, 707 North Broadway, Baltimore, MD 21205; e-mail: Naidu@kennedykrieger.org

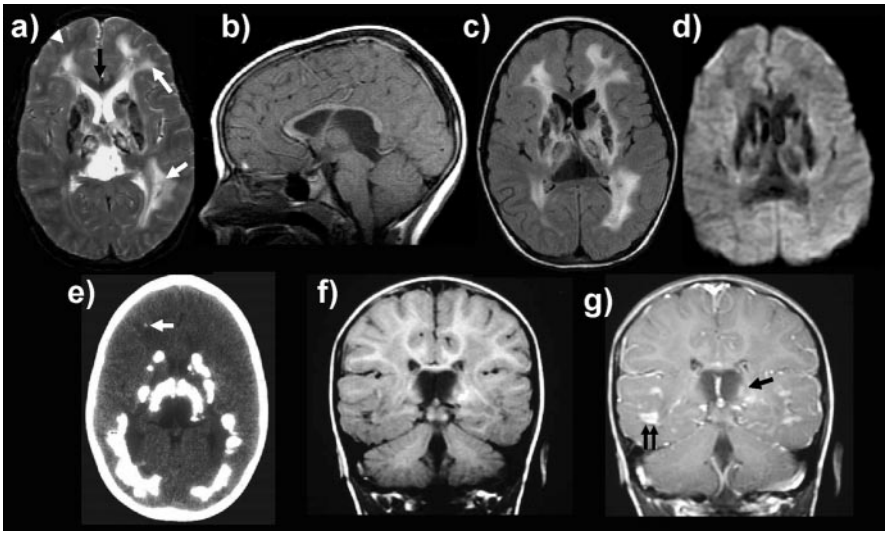

Figure 1. Patients 1 (E–G) and 2 (A–D): axial T2-weighted image (A) shows white matter hyperintensity (white arrows). Note sparing of U fibers (white arrowhead) and corpus callosum (black arrow), also seen on sagittal T1-weighted (B). Axial fluid-attenuated inversion recovery image (FLAIR) (C) confirms the cystic nature of the interhemispheric lesion. Axial diffusion-weighted image (D; repetition time/echo time, 10,000/120 ms; three orthogonal gradient directions; single-shot spin-echo echo-planar imaging (SE EPI); and b_{max}, 1000 s/mm^2) shows no water restriction in the cyst or parenchyma. Nonenhanced CT (E) shows extensive and coarse calcifications in the basal ganglia, thalamus, and parietal white matter. Note subtle calcification in the central white matter on the right frontal lobe (white arrow). Coronal T1-weighted images pregadolinium (F) and postgadolinium (G) show lack of enhancement in the interhemispheric cyst and subtle enhancement adjacent to it (black arrow) and within some calcifications (double black arrows).

DWI showed no restriction (see figures 1D and 2.IF) in the cysts and affected white matter. In Patient 2, the cyst showed elevated apparent diffusion coefficient (ADC) values ($2.94 \pm 0.23 \times 10^{-9}$ m^2/s), close to the values obtained from the CSF in the lateral ventricles ($3.14 \pm 0.16 \times 10^{-9}$ m^2/s). Increase in ADC values were also appreciated in the affected white matter ($1.74 \pm 0.01 \times 10^{-9}$ m^2/s) and adjacent normal-appearing white matter ($0.91 \pm 0.06 \times 10^{-9}$ m^2/s). Gray matter ($0.88 \pm 0.02 \times 10^{-9}$ m^2/s) had slightly low values. Normal values for white matter (0.76 ± 0.09 to $0.82 \pm 0.07 \times 10^{-9}$ m^2/s) and gray matter (0.96 ± 0.10 to $1.03 \pm 0.08 \times 10^{-9}$ m^2/s) were obtained from the literature.[3]

Discussion. The uniformity of MRI findings in our three patients with clinical variation beyond that described previously broadens the phenotype of this disorder, encompassing features of Coats disease (Patient 1).

Patient 2's normal brain CT early in life indicates postnatal evolution of the calcifications and cysts.

The areas of subtle gadolinium enhancement observed in our patients could reflect the microangiopathy previously reported from surgical specimens.[1] Normal angiography and MRA studies obtained from Patient 1 and also previously described do not exclude this possibility because these imaging modalities are expected to detect major and medium vessel abnormalities and not small vessel pathology, as is

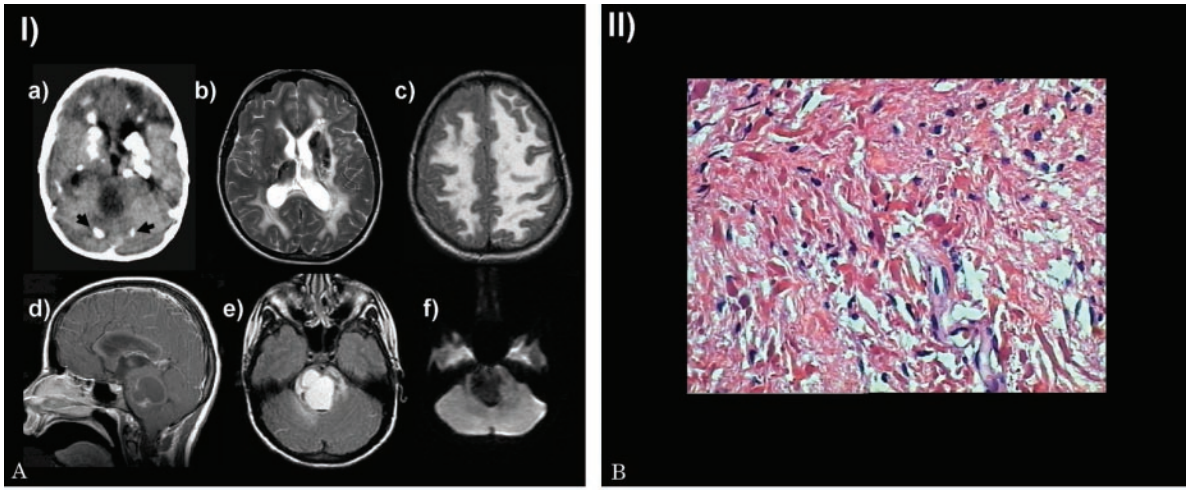

Figure 2. Patient 3. I. Nonenhanced CT (A) shows calcifications in the cerebellum and dentate nuclei (black arrow). Note the posterior fossa midline cyst. Axial T2-weighted image (B) shows calcifications and white matter hyperintensity. Axial fluid-attenuated inversion recovery image (FLAIR) (C) shows extensive white matter abnormalities. Sagittal postgadolinium T1-weighted image (D) shows enhancement around the cyst. Axial FLAIR (E) shows high signal in the cyst, reflecting high protein content, although diffusion-weighted image (F) shows no water restriction (hyposignal). II. Fibroglial tissue with conspicuous formation of Rosenthal fibers; H-E, ×400.

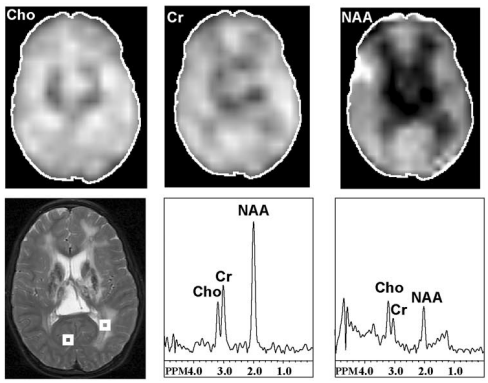

Patient 2. MRSI: metabolite concentrations (mM) and ratios

	[NAA]	[Cho]	[Cr]	[NAA/Cho]	[NAA/Cr]	[Cho/Cr]
Frontal white matter	5.5±0.87 (7.77±0.56)	1.65±0.40 (1.74±0.25)	6.40±1.74 (5.75±2.51)	1.53±0.24 (1.99±0.35)	1.84±0.36 (3.14±1.41)	1.22±0.25 (1.63±0.81)
parietal white matter	3.95±1.58 (7.56±0.67)	1.27±0.23 (1.68±0.23)	5.07±1.62 (4.82±0.89)	1.43±0.52 (2.03±0.14)	1.59±0.39 (3.25±0.57)	1.18±0.28 (1.62±0.38)
Frontal gray matter	6.69±1.27 (7.19±1.38)	1.32±0.34 (1.33±0.28)	6.92±1.45 (4.83±1.78)	2.19±0.31 (2.42±0.41)	2.10±0.66 (3.12±0.64)	0.95±0.23 (1.32±0.35)
parietal gray matter	6.24±0.92 (7.50±0.59)	1.28±0.14 (1.61±0.12)	7.13±0.90 (5.61±0.80)	2.12±0.25 (2.12±0.26)	1.84±0.37 (2.72±0.29)	0.86±0.11 (1.30±0.24)

Figure 3. Patient 2. Magnetic resonance spectroscopy study. Four supratentorial, 15-mm-thick slices (repetition time/echo time, 2,800/280 ms; field of view, 24 cm; matrix size, 32 × 32; and 0.8 cm^3 voxel size). Metabolite maps in the top row show overall reduction of metabolites, particularly N*-acetylaspartate. No metabolites are seen in the calcifications. In the bottom row, two examples of spectra obtained for the white (right) and gray (center) matter in the posterior parietal region are demonstrated, with voxel location shown on the left. Table: Results displayed as average and SD of 6 voxels in each location; normal values of two age- and sex-matched control subjects ± SD are displayed in parenthesis for comparison.*

the case here. Biopsy from Patient 3 showed ferric iron deposits in macrophages, possibly reflecting previous hemorrhage, and partially calcified vessels. Absence of angiomatous changes may have been due to a small tissue sample that included a fragment of the cyst wall and not the surrounding white matter.

MRS, not previously described, showed reduction of NAA and Cho, consistent with increase in water content, as opposed to a demyelinating process, in which high Cho levels would be expected. High Cr concentrations not exceeding 2 SD in the context of our small sample preclude unequivocal interpretation, but one possibility could be the presence of gliosis, previously described in this disease. No metabolites were detected in the cysts or within the calcifications. Despite differences in MRS protocols and data analysis at the two separate institutions, control values used for comparison were obtained within each institution.

DWI showed no restricted diffusion, and ADC values demonstrated higher diffusivity, reflecting tissue damage compatible with increased water content in abnormal- and normal-appearing white matter.[4] MRS and DWI results concur with the proposed etiology for the cysts presumed to originate from progressive increase of fluid content in the white matter lesions after necrosis. Perhaps because of inflammatory or vascular abnormalities, some of these cysts enlarge to cause obstructive hydrocephalus.

Our patients have clinical and radiologic features similar to LCC, except for the retinal, skin, and hair abnormalities of Patient 1.[1] A previous report showed two siblings[5] with sparse hair, dysmorphic features, brain calcifications, and Coats disease, a vascular retinal entity.[6] Although not specified in this publication, the siblings also had leukoencephalopathy (Dr. J.B.P. Stephenson, personal communication). Another report described progressive basal ganglia calcifications, leukoencephalopathy, and bilateral Coats disease and noted that the similarities in angiomatous changes in their patients and those with LCC suggested a possible relationship between them.[7] However, they also noted that their subjects lacked cerebral cysts, and there were no reported retinal abnormalities in those with LCC. Our Patient 1 had Coats disease in addition to LCC features, which suggests a link between these two conditions and warrants consideration of a broader clinical spectrum. Consanguinity in parents of one patient and occurrence in siblings suggest autosomal recessive inheritance.[5]

Acknowledgment

The authors thank Dr. J.B.P. Stephenson, Royal Hospital for Sick Children, Glasgow, Scotland, for helpful comments; Dr. Ann Tournay, UCLA, for CT scan and retinal pictures of Patient 1; Dr. Christine R. Gonzales, Stein Eye Institute, UCLA, and Dr. Yossi Sidikaro, Beverley Hills, for evaluation and treatment of Patient 1; and Dr. Maria Conception Garcia Otaduy, Hospital das Clínicas da Faculdade de Medicina da Universidade de São Paulo, Brazil, for helping with MRS data from Patient 3.

References

1. Labrune P, Lacroix C, Goutieres F, et al. Extensive brain calcifications, leukodystrophy, and formation of parenchymal cysts: a new progressive

disorder due to diffuse cerebral microangiopathy. Neurology 1996;46: 1297–1301.
2. Duyn JH, Gillen J, Sobering G, van Zijl PC, Moonen CT. Multisection proton MR spectroscopic imaging of the brain. Radiology 1993;188:277–282.
3. Morriss MC, Zimmerman RA, Bilaniuk LT, Hunter JV, Haselgrove JC. Changes in brain water diffusion during childhood. Neuroradiology 1999; 41:929–934.
4. Pierpaoli C, Righini A, Linfante I, Tao-Cheng JH, Alger JR, Di Chiro G. Histopathologic correlates of abnormal water diffusion in cerebral ischemia: diffusion-weighted MR imaging and light and electron microscopic study. Radiology 1993;189:439–448.
5. Tolmie JL, Browne BH, McGettrick PM, Stephenson JB. A familial syndrome with Coats' reaction retinal angiomas, hair and nail defects and intracranial calcification. Eye 1988;2:297–303.
6. Manschot WA, de Bruijn WC. Coats' disease: definition and pathogenesis. Br J Ophthalmol 1967;51:145–157.
7. Goutieres F, Dollfus H, Becquet F, Dufier JL. Extensive brain calcification in two children with bilateral Coats' disease. Neuropediatrics 1999; 30:19–21.